The Perception of Static Colored Noise: Detection and Masking Described by CIE94

Marcel P. Lucassen,[1]* Piet Bijl,[1] Jolanda Roelofsen[2]

[1] TNO Human Factors, Soesterberg, The Netherlands

[2] Cognitive Psychology, Vrije Universiteit, Amsterdam, The Netherlands

Received 7 March 2007; revised 29 June 2007; accepted 2 August 2007

*Abstract: We present psychophysical data on the perception of static colored noise. In our experiments, we use the CIE94 color difference formula to quantify the noise strength and for describing our threshold data. In Experiment 1 we measure the visual detection thresholds for fixed pattern noise on a uniform background color. The noise was present in one of three perceptual color dimensions lightness (*L*), chroma (*C*), or hue (*h*). Results show that the average detection threshold for noise in* L* *is independent of hue angle and significantly lower than that for noise in* C* *or* h. *Thresholds for noise in* C* *and h depend on hue angle in an opponent fashion. The measured detection thresholds, expressed in terms of the components* $\Delta L^*/k_L S_L$, $\Delta C^*/k_C S_C$, *and* $\Delta H^*/k_H S_H$ *that build up the CIE94 color difference formula are used to tune CIE94 to our experimental conditions by adjusting the parametric scaling factors* k_L, k_C, *and* k_H. *In Experiment 2, we measure thresholds for recognizing the orientation (left, right, up, down) of a test symbol that was incremental in* L*, C*, *or* h, *masked by supra-threshold background noise levels in* L*, C*, *or* h. *On the basis of the CIE94 color difference formula we hypothesized (a) a constant ratio between recognition threshold and noise level when the test symbol and background noise are in the same perceptual dimension, and (b) a constant recognition threshold when in different dimensions. The first hypothesis was confirmed for each color dimension, the second however, was only confirmed for background noise in* L*. *The* L*, C*, h *recognition thresholds increase with increasing background noise in* C* *or* h. *On the basis of some 16,200 visual observations we conclude that the three perceptual dimensions* L*, C*, *and* h *require different scaling factors (hue dependent for* C* *and* h*) in the CIE94 color difference formula, to predict detection threshold data for color noise. In addition these dimensions are not independent for symbol recognition in color noise.* © 2008 Wiley Periodicals, Inc. Col Res Appl, 33, 178–191, 2008; Published online in Wiley InterScience (www.interscience.wiley.com). DOI 10.1002/col.20401

Key words: psychophysics; CIE94 color difference; detection threshold; chromatic discrimination; noise masking

INTRODUCTION

Differences between color samples are generally expressed in terms of the CIELAB based ΔE metric for which a number of industrial standards have been issued over the years: CIELAB,[1] CMC,[2] CIE94,[3] and CIEDE2000.[4] Under supervision of the Commission Internationale de l'Éclairage (CIE) the mathematical equations underlying the calculation of ΔE—known as *color difference formulae*—are still being refined. These formulae are tuned to an ever increasing number of data sets obtained from human observers in vision experiments employing specific stimulus sizes and viewing conditions, the so called *reference conditions*. When applying such a color difference equation however, one should be aware of its preferred reference conditions, and hence its limitations for some practical cases. For instance, it is required that the two color samples for which the ΔE is calculated are uniform and of considerable spatial dimension (4° visual angle minimum). Compared to the number of color difference studies involving uniform colors, systematic research on models for describing the perception of differences between nonuniform (textured) colors has only just begun.

*Correspondence to: Marcel P. Lucassen, Lucassen Colour Research, Amsterdam, The Netherlands (e-mail: marcel@lucr.nl).

Adding texture to homogeneous color samples increases lightness tolerance thresholds by a factor of almost two.[5,6] It was also shown how texture increases the parametric factors in the color difference formula for lightness, chroma, and hue.[7] On the scale of images, rather than the scale of samples, a spatial extension of the CIELAB color difference formula for evaluation of differences in image pairs (e.g., the difference between an original image and a compressed version) has been developed.[8]

In the present study, we investigate the visual system's performance on the detection of static colored noise, i.e., spatial variations around an average in one of three basic dimensions for color perception. In addition, we study the recognition of a test symbol masked by different amounts of this "background" noise. The rationale for these experiments is our interest in the development of models for predicting the performance of a human observer who needs to detect or identify a target in a noisy image. We here mention two classes of applications. First, there are a number of color vision tests that make use of pseudo-isochromatic test plates (like the well-known Ishihara color vision test). These plates contain test symbols that are detected by color normals on the basis of a chromatic difference between test symbol and background. The purpose of these tests is that color blinds fail to detect some of the test symbols so that their deficiency can be traced. To prevent that color blinds can still see the test symbol on the basis of a luminance difference (for instance, protans perceive red colors as more dark), the test symbol is embedded in a "noisy" luminance pattern.[9] Threshold measurements for these test symbols are crucial for the design of color vision tests. Second, another class of examples is related to multi-spectral imaging systems. These systems combine information from different spectral bands (e.g., in the visible, infrared, and/or the ultra-violet regions of the spectrum) and so allow for the creation of fused false-color images in which both *signal* (a target against a background) and *noise* of different chromatic content are present. Understanding the basic mechanisms underlying the perception of colored noisy images is required in order to be able to (a) predict the performance of a human observer on target detection or recognition[10,11] and (b) design false-coloring schemes that optimally support these tasks.

The CIE94 Color Difference Formula as Our Yardstick for Color Noise

For the specification of the amount of pattern noise and the strength of the test symbol in our experiments we make use of the CIE94 color difference formula, thereby deliberately and systematically deviating from the preferred reference conditions. Although there is a more recent color difference formula available,[4] we intentionally work with the 1994 version, mainly because of its simplicity and symmetry, but also because of practical issues related to implementation of the formula into our software for generating the stimuli. However, we do present a comparison of the CIE94 results with the CIEDE2000 formula. The CIE94 color difference formula is given by[†]

$$\Delta E^*_{94} = \sqrt{\left(\frac{\Delta L^*}{k_L S_L}\right)^2 + \left(\frac{\Delta C^*_{ab}}{k_C S_C}\right)^2 + \left(\frac{\Delta H^*_{ab}}{k_H S_H}\right)^2} \qquad (1)$$

in which the components $\Delta L^* = L^*_1 - L^*_2$, $\Delta C^* = C^*_1 - C^*_2$, and $\Delta H^* = H^*_1 - H^*_2$, calculated for two color samples 1 and 2, are weighted with functions S_L, S_C, S_H, and parametric factors, k_L, k_C, k_H. The weighting functions are defined by

$$\begin{aligned} S_L &= 1 \\ S_C &= 1 + 0.045\,C^* \\ S_H &= 1 + 0.015\,C^* \end{aligned} \qquad (2)$$

As Eq. (2) shows, the weighting functions S_C and S_H depend on the average chroma (C^*) of the two color samples for which the color difference is computed. The CIE established a set of reference conditions under which the CIE94 color difference equation performs well.[3] The parametric factors, k_L, k_C, k_H in Eq. (1) are used to adjust the relative weighting of the lightness, chroma, and hue components for various viewing conditions and applications that differ from the reference conditions. Under the reference conditions the k-factors are set to unity.

Our research consists of two main experiments and a number of pilot studies.[12,13] Because we planned to deviate from the reference conditions throughout the research, it was necessary to determine the parametric factors k. In our first experiment (Experiment 1) we measure the threshold level of static noise in terms of ΔE^*_{94}. This was done for noise in the three directions, L^*, C^*, and h separately.[‡] When selecting one direction, the Δ-components of the other two remain 0, which simplifies Eq. (1) to the following three cases:

$$\Delta E^*_{94} = \left(\frac{\Delta L^*}{k_L S_L}\right) \qquad \Delta C^* = \Delta H^* = 0 \qquad (3)$$

$$\Delta E^*_{94} = \left(\frac{\Delta C^*}{k_C S_C}\right) \qquad \Delta L^* = \Delta H^* = 0 \qquad (4)$$

$$\Delta E^*_{94} = \left(\frac{\Delta H^*}{k_H S_H}\right) \qquad \Delta L^* = \Delta C^* = 0 \qquad (5)$$

In the second experiment (Experiment 2) the visibility of a test symbol (a square U) in the presence of different amounts of noise was studied. The parametric factors k_L, k_C, k_H were first assigned the threshold values for the noise as measured in Experiment 1 to let the threshold correspond to $\Delta E^*_{94} = 1$. Both the test symbol and the noise were independently addressed in lightness (L^*), chroma (C^*), or hue (h), so nine combinations in total. It was expected that when the directions of the color signals are the same for test symbol and noise, the ratio between recognition threshold and noise level is constant. How-

[†] In the remaining we shall omit the subscripts ab in C^*_{ab} and H^*_{ab}.

[‡] In this study we use the symbol h to indicate a direction in color space (hue), but also to indicate the hue angle (i.e., a value in degrees).

ever, the noise level should not affect the perception of the test symbol when the directions are different.

METHODS

Our experiments required a great deal of technical preparations, mostly in software. We refer to the Appendix where our approach to the problem of display calibration, color resolution, and color selection are presented in detail.

Experimental Set-up

In a darkened room, subjects were seated at a 50 cm viewing distance from an 18-inch LCD on which the stimuli were presented. The display, an Eizo ColorEdge CG18, had a native resolution of 1280 × 1024 pixels and a 0.28 mm pixel dot size. Refresh rate was 60 Hz. Custom software for generating and presenting the stimuli was running on an Intel Pentium 4 computer with a 2.40 GHz processor and a 24-bit color resolution graphics card (Matrox Parhelia). As detailed in the Appendix, we increased the color resolution in software from 24 to 33 bits by the technique of low contrast spatial dithering.

Stimuli

Two examples of the stimuli used in the experiments are shown in Fig. 1. Each display consisted of four quadrants, one of which contained the test stimulus that had to be detected by the observers. With each new stimulus presentation, the test stimulus was randomly assigned to one of the four quadrants. The quadrants were in turn subdivided in smaller squares (0.58° each) that were individually addressed with a color specification in terms of L^*, C^*, and h.

In Experiment 1 the quadrants were made up of 625 (25 × 25) smaller squares, showing a common colored background and one quadrant contained additional noise (see Fig. 1, left side). The amount of noise was set by the value of ΔE^*_{94} and was under the control of a staircase procedure (to be explained). The noise was applied in one of the three perceptual directions L^*, C^*, or h, but not simultaneously in two or three. Each small square was randomly assigned +1, 0, or −1 times the noise level specified by ΔE^*_{94}. What this means in terms of L^*, C^*, and h depends on the selected noise direction and the values for the scaling factors (k and S) in Eqs. (3)–(5). In any case, the scene-averaged L^*, C^*, h values of the quadrant with noise are identical to those of the quadrants without noise. The maximum difference between two neighboring squares was 2 ΔE^*_{94}.

In Experiment 2 the quadrants were made up of 784 (28 × 28) small squares, showing a colored background with noise and an additional test symbol (a square U) with one of four possible orientations (up, down, left, right). All quadrants contained a different symbol orientation. Subjects had to look for the quadrant containing the symbol in the up-orientation. The test symbol was about one-third the size of the quadrant, and incremental to the background noise, i.e., with higher values for the selected color direction (either L^*, C^*, or h). Since the color direction of the background noise and the color direction of the incremental test symbol can be independently selected to be L^*, C^*, or h, nine possible combinations of the color directions exist, all of which we studied. Examples of these combinations are shown in Fig. 2.

Threshold Definition

A four-alternative-forced-choice (4AFC) procedure was implemented in a staircase method for measuring the

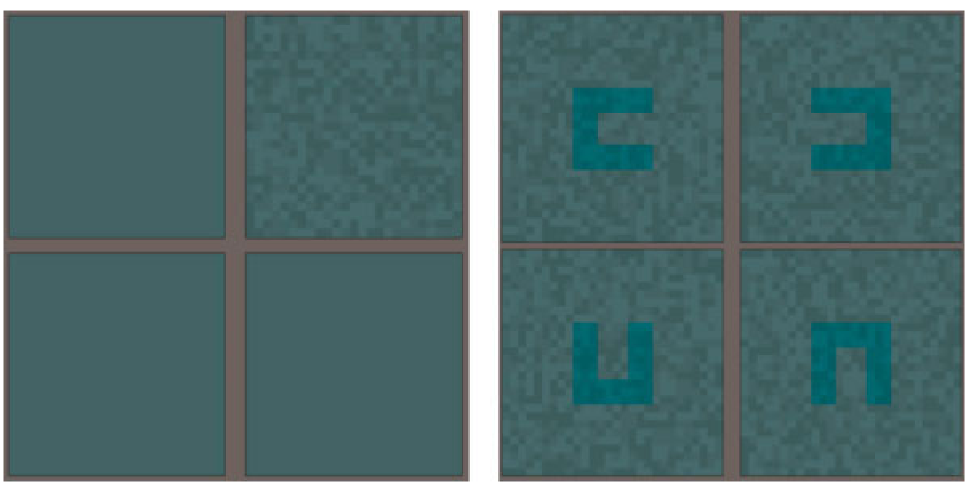

FIG. 1. Examples of the stimuli used in Experiment 1 (left) and Experiment 2 (right). At the viewing distance of 0.5 m each quadrant subtended a visual angle of 14.5° (Experiment 1) or 16.2° (Experiment 2). In the two examples the background color is at $L^* = 50$, $C^* = 20$, $h = 180$ and the background noise is in direction L^*. The additional U-shaped symbol in Experiment 2 is incremental in C^*, i.e., at a higher saturation level. Subjects had to look for the test stimulus, being the quadrant containing noise in Experiment 1 or the quadrant containing the U-symbol in up-orientation in Experiment 2.

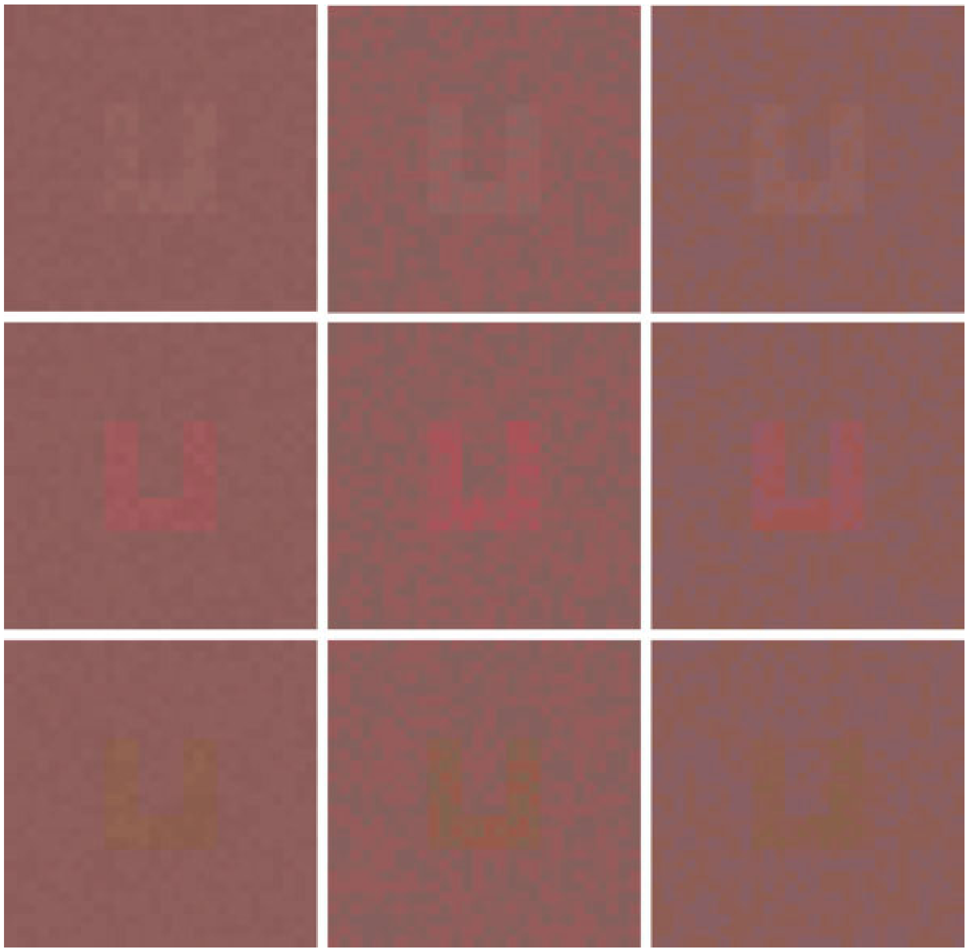

FIG. 2. Overview of the nine possible combinations of the color directions for background noise and test symbol, as studied in Experiment 2. Left to right: background noise in L^*, C^*, h. Top to bottom: Test symbol increment in L^*, C^*, h. Shown are the examples with $L^* = 50$, $C^* = 20$, and $h = 0$. In these examples the strength of the noise and test symbol increment was set at 15 and 30 times the threshold levels for the perception of the background noise (due to limited color reproduction accuracy, the effects may be less well pronounced in print). Also note that in this figure the test-symbols are all presented in the up-orientation.

visual threshold of the test stimuli. Each stimulus presentation consisted of four quadrants. Subjects had to indicate the quadrant that—according to their perception—contained the test stimulus. In Experiment 1 the test stimulus contained noise (the upper right quadrant in the example of Fig. 1) whereas in Experiment 2 it contained the U-shaped symbol in the up-orientation (the lower left quadrant in the example of Fig. 1). In Fig. 3 an example of the staircase is presented. It shows how the stimulus strength [in terms of the metric ΔE^*_{94} as in Eqs. (3)–(5)] is decreased after two successive correct responses and how it is increased after one incorrect response. When the sign of the strength adjustment is changed, a reversal arises. After 10 reversals the staircase procedure was terminated and the final threshold was computed as the average of the strength values associated with the last six reversals.

As a rule-of-thumb a strength adjustment of 0.06–0.1 log units gives optimal results.[14] Table I shows the strength adjustments applied in our experiments. It can be shown that this procedure yields ~75% correct

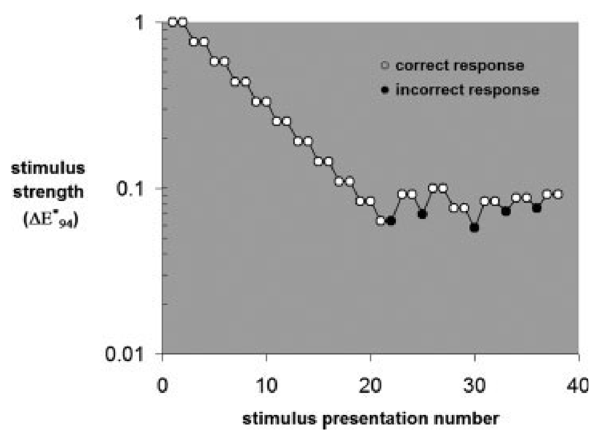

FIG. 3. Example of stimulus strength adjustment with the staircase method. Note the logarithmic vertical scale. In Experiment 1, the stimulus strength corresponds to the amplitude of incremental and decremental noise on a uniform background color, in Experiment 2 it corresponds to the amplitude of an incremental test symbol. See Table I also for details on the adjustments after two successive correct responses or one incorrect response.

TABLE I. Adjustments in stimulus strength in the 4AFC staircase procedure (see Fig. 3 also).

	Decrease in $\log(\Delta E^*_{94})$	Increase in $\log(\Delta E^*_{94})$	During
After two successive correct responses	0.12	–	First six reversals
	0.06	–	Last four reversals
After one incorrect response	–	0.16	First six reversals
	–	0.08	Last four reversals

answers,[14,15] which means that 2/3 (66.6%) of the test stimuli are really seen. From the remaining 1/3 of the test stimuli (not seen), 1/4 is correctly guessed on average. So, in total 66.6% + ¼(33.3%) = 75%. This was confirmed by our pilot data.

Observers

Three subjects participated in the experiments, one male and two females, age ranging from 23 to 39. They all had normal color vision as confirmed by different color vision tests (Ishihara, Farnsworth D15 and the TNO VisionScreener,[16] and normal or corrected to normal visual acuity. The subjects worked or were in training at the institution where the experiments were carried out and did not get paid for their participation. All subjects were familiar with the purpose of the experiments. However, because the measurement procedure incorporates a 4AFC method for establishing the visual thresholds it is not expected that this may have influenced the results.

Experimental Procedure

Subjects were instructed to sit 50 cm from the LCD (we did not want to use a chin rest). The center of the display was at eye level and subjects were straight in front of the display. During experimental sessions the room was darkened. Before the session a color calibration was carried out (see color calibration section). Also, a suitable starting value for ΔE^*_{94} in the staircase procedure was determined by visual inspection of the stimulus preview. This was necessary to guarantee an initial stimulus display that was well above threshold and allowed the subjects to get familiar with the stimulus condition. Observer JR used starting values of $\Delta E^*_{94} = 1$ for all conditions. Observer ML used a starting value $\Delta E^*_{94} = 1$ for thresholds in L^*, and average starting values (averaged over hue angles) of 1.08 and 1.62 for C^* and h, respectively. Observer NL used average starting values of 1.54, 1.85, and 2.38 for L^*, C^*, and h, respectively. The task of the subjects was to indicate the quadrant containing the test stimulus (Fig. 1). This was done by pressing the space bar of the keyboard, which moved a marker from one quadrant to the next, and the enter-key was pressed to confirm the quadrant selection. After a wrong response the subjects heard a beep. This feedback has a stabilizing effect because at threshold level subjects may become insecure about their performance. There was no time restriction, and subjects could work at their own speed. One trial took about 3 min in Experiment 1 and about 5 min in Experiment 2. Experimental sessions lasted for about 1 h, at maximum. In total, 16,200 responses were recorded.

RESULTS

Experiment 1: Detection Thresholds of L^*, C^*, h Noise

In Experiment 1, thresholds for the detection of background noise in the separate directions L^*, C^*, and h were measured in terms of ΔE^*_{94}. We selected the values $L^* = 50$ and $C^* = 20$ as our standard working point and set the parametric factors k_L, k_C, k_H at 1. With these values we could still manipulate the stimuli along the L^*, C^*, and h axes without exceeding the boundaries of the LCD's color gamut. The hue axis was sampled at 30° intervals.

In Fig. 4 the individual results are shown for the three subjects. Comparison of their data sets reveals a consistent behavior of the thresholds with varying hue angle. Statistical analysis showed that there was no significant difference between subjects. Independent *t*-tests were carried out on subject pairs (equal variances between subjects), separately for the directions L^*, C^*, and h. Since we found no significant differences between subjects we averaged the thresholds for each perceptual direction over subjects, as shown in Fig. 5.

The data contain the following important features:

1. The threshold for the detection of noise in L^* is considerably lower than that for the other two directions, and practically independent of hue angle.
2. The thresholds for the detection of noise in C^* and h show a clear dependency on hue angle, and in an opponent fashion, i.e., when the threshold for noise in C^* is high, the threshold for noise in h is low, and vice versa.
3. The threshold for noise in h shows a pronounced peak at a hue angle of 240°.

Altogether, the data show that for our experimental conditions the CIE94 color difference formula with the parametric factors set to 1 is far from uniform. Ideally, one would like to have a formula that is perceptually uniform in all directions, so that a $\Delta E = 1$ evoked by a ΔL is perceived equally large as $\Delta E = 1$ evoked by a ΔH or ΔC (including their respective weighting factors). The CIE has adopted a more recent color difference formula[4,17] than the 1994 version we used for specifying color differences. In addition to the three components of Eq. (3) the CIEDE2000 color difference formula also contains an interaction term between chroma and hue, which might take care of the interaction (opponency) between our C^* and h threshold data. In the graph on the right

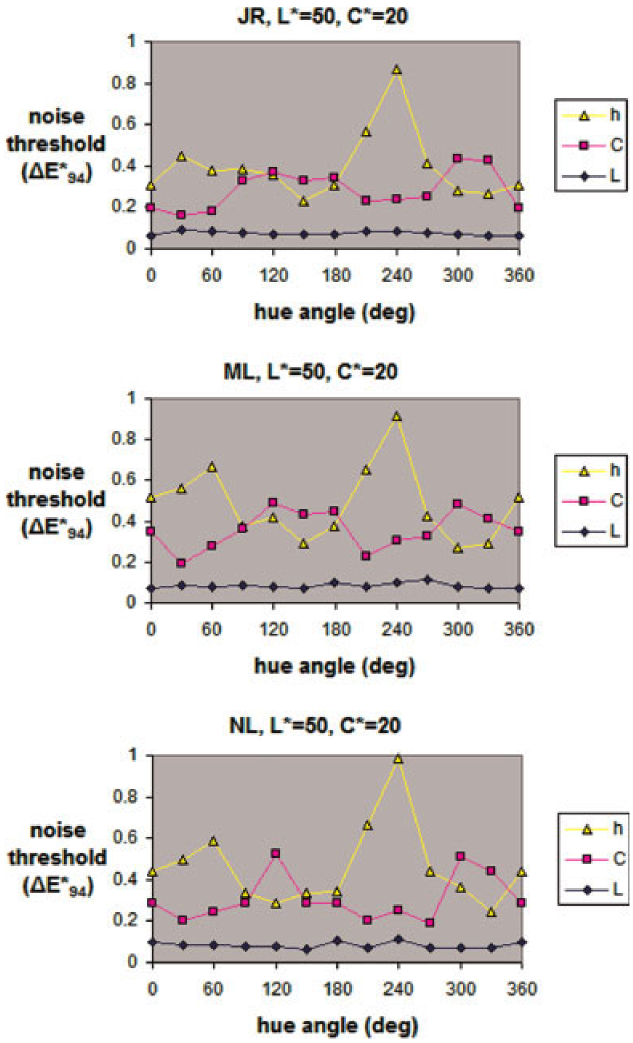

FIG. 4. Detection thresholds with varying hue angles. Results of Experiment 1 for three subjects (top to bottom: JR, ML, NL) at $L^* = 50$ and $C^* = 20$. The noise threshold (vertical axis) is the value resulting from the 4AFC staircase method and indicates 75% correct detection of the noise pattern. Noise was present in either L^*, C^*, or h as indicated by the legend. Data points at $h = 360$ are copied from $h = 0$. [Color figure can be viewed in the online issue, which is available at www.interscience.wiley.com.]

hand side in Fig. 5, we replotted our threshold data in terms of the ΔE_{00} color difference metric. Compared to the left hand graph, the data look much the same however. Most prominent difference is the increase in peak height for the threshold in h at $h = 60°$. So, the CIEDE2000 formula does not provide a more convenient description of our data. We will provide more comments on the results of Experiment 1 in the Discussion.

Experiment 2: Symbol Recognition in Noisy Background

In our second experiment the goal was to measure the thresholds for recognizing the orientation of a U-shaped test symbol that was superimposed (incremental) on the background noise. These increment thresholds were determined for the separate directions L^*, C^*, and h. Since both the background noise and the test symbol were separately controlled, in total nine combinations of the noise direction and the test symbol direction were studied (see the examples in Fig. 2). Before running the actual experimental sessions, the parametric factors k_L, k_C, k_H in Eqs. (3)–(5) were set equal to the threshold values measured in Experiment 1. Since these varied for the different subjects and for the different hue angles (see Fig. 4), each subject used his/her own set of values. There are two reasons for applying these scale factors. First, the result is that $\Delta E^*_{94} = 1$ now corresponds to 1 just noticeable difference (JND), and $\Delta E^*_{94} = 2$ corresponds to 2 JND, etc. (we define 1 JND as the 75% correct threshold). This greatly simplifies the interpretation of the results of Experiment 2. Second, as long as the noise does not simultaneously address two or three of the perceptual directions, 1 JND in L^* also corresponds to 1 JND in C^* and to 1 JND in h (the same restriction holds for the test symbol).

The background noise was the independent variable with levels of $\Delta E^*_{94} = 0$, 5, 10, 15, and 20, (i.e., at 0, 5, 10, 15, and 20 times the threshold) at $L^* = 50$, $C^* = 20$, and $h = 0$.

In Fig. 6 the results of Experiment 2 are shown as obtained for $L^* = 50$, $C^* = 20$, and $h = 0$, averaged over

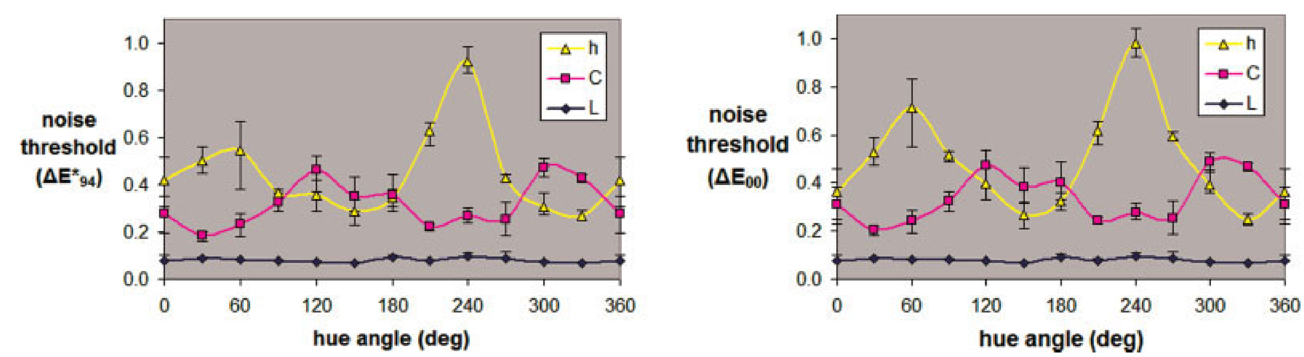

FIG. 5. Results of Experiment 1, averaged over subjects. The graph on the left shows the noise detection thresholds in terms of ΔE^*_{94}, the one on the right in terms of the more recent ΔE_{00} color difference metric. The vertical bars indicate the full range, including the minimum and maximum data point. Note the lower thresholds for L^*, the opponent behavior of C^* and h, and the pronounced peak for h at $h = 240°$. [Color figure can be viewed in the online issue, which is available at www.interscience.wiley.com.]

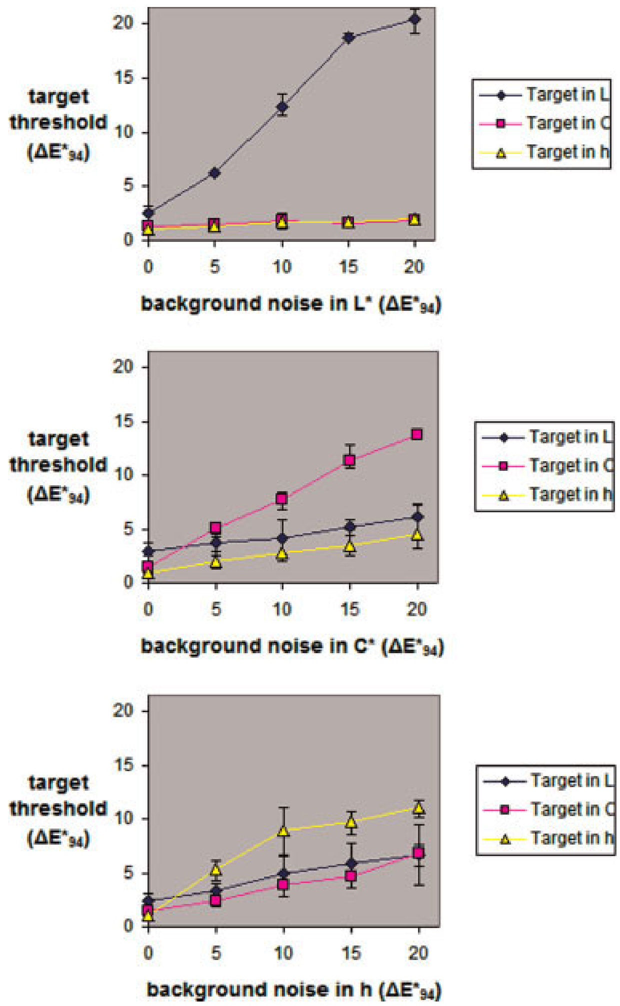

FIG. 6. Results of Experiment 2, averaged over subjects. Vertical bars indicate the full range, including the minimum and maximum data point. Vertical axis plots the threshold for 75% correct recognition of the orientation of the incremental U-shaped test symbol that was masked by background noise (horizontal axis). Top to bottom: background noise in L^*, C^*, h, respectively. Results obtained for $L^* = 50$, $C^* = 20$, $h = 0$. See text for further discussion. [Color figure can be viewed in the online issue, which is available at www.interscience.wiley.com.]

the three subjects. The range over which the individual measurements varied is indicated by the vertical bars. Figure 6 shows that when the background noise is in L^* (top panel), the recognition threshold for the test symbol in L^* increases almost linearly with the amount of background noise. Linear regression reveals a slope of 0.97, $R^2 = 0.97$. In contrast, the thresholds for the target in C^* or h are independent of the background noise in L^*. This was the expected result.

When comparing the results for the background noise in C^* (middle panel) with those for the background noise in L^*, three observations are worth mentioning. First, the slope of the recognition threshold for the test symbol in C^* is 0.62 ($R^2 = 0.99$), which is smaller than the slope of the L^*-curve (0.97) with background noise in L^*. Second, the slopes of the two "other" target directions (L^* and h) are slightly positive. Third, these two target directions also differ in their dependency on the background noise (the target in h is more easily recognized than the target in L^*).

When comparing the results for the background noise in h with those for the background noise in C^*, two observations are worth mentioning. First, the slope of the recognition threshold for the test symbol in h is 0.48 ($R^2 = 0.91$), somewhat smaller than the slope of the C^*-curve (0.62) with background noise in C^*. Second, the slopes of the two "other" target directions (L^* and C^*) are slightly more positive.

In Fig. 7 we replotted some of the data of Fig. 6, for the conditions in which the perceptual dimensions of the target and the masking noise were identical. Interestingly, the figure shows that L^*-thresholds are consistently larger than the C^* and h thresholds. This indicates that chromatic signals (in C^* or h) in chromatic noise are better detected than achromatic signals in achromatic noise. Detailed analysis of this subject and its potential advantages for practice will be discussed later.

Statistical analysis of the data in Fig. 7 was done in the following way. Since the three curves share the same x-values (background noise), we calculated the differences between L^* and C^*, L^* and h, and C^* and h. Then, linear regressions on the data points of these three sets of differences were performed. The results lead to the conclusion that significant differences exist between L^* and C^* and L^* and h at the 97.5% confidence level. However, there is no significant difference between C^* and h at the 90% or higher confidence level. In other words, the slopes of the C^* and h curves in Fig. 7 are significantly smaller than the slope of L^*, and the slopes of C^* and h are equal.

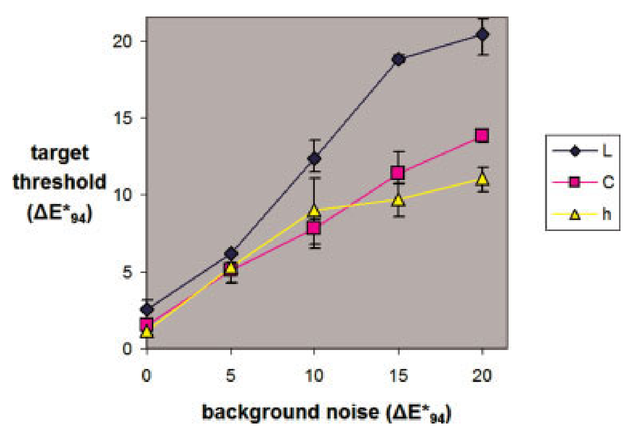

FIG. 7. Results of Experiment 2, for the conditions in which the target and the masking noise are in the same dimension (replotted from Fig. 6). Note that the threshold curves for C^* and h lie below the threshold curve for L^*, indicating that chromatic signals may be detected more efficiently than achromatic signals. [Color figure can be viewed in the online issue, which is available at www.interscience.wiley.com.]

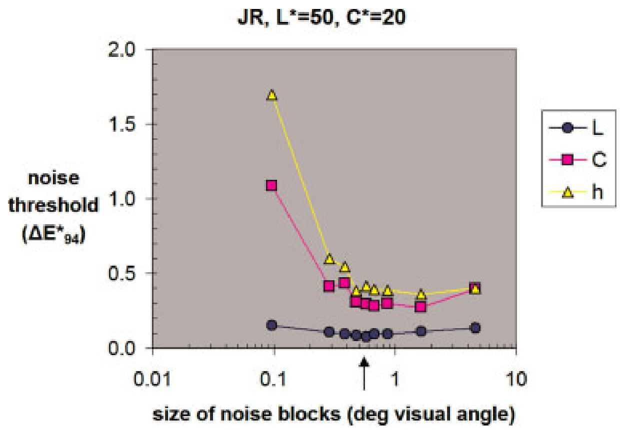

FIG. 8. Detection thresholds for background noise at different sizes of the noise blocks that build up the stimulus. The size of the noise blocks is given in degrees visual angle. The arrow on the horizontal axis indicates the resolution that was used in the main Experiments 1 and 2. Shown here are the data for observer JR, averaged over the six hue angles. See Table II for the data at individual hue angles. Note how the threshold increases for smaller block sizes. [Color figure can be viewed in the online issue, which is available at www.interscience.wiley.com.]

Effect of Spatial Resolution

To study the effect of spatial resolution on the detection threshold of static background noise in L^*, C^*, or h, we repeated Experiment 1 for different sizes of the small "noise squares" (see Fig. 2). The parametric factors in Eqs. (3)–(5) were again set at unity. The hue angle was sampled at 60° intervals, and $L^* = 50$, $C^* = 20$. Because of the technique of spatial dithering that we applied for increasing the color resolution, the sides of the squares could only be a multiple of 3 pixels. We used square sides of 3, 9, 12, 15, 18, 21, 27, 51, and 144 pixels. Given the 0.28 mm display pixel pitch and the 50 cm viewing distance 1 pixel subtended a visual angle of 0.032°, meaning that for our smallest block size (sides of 3 pixels) the visual angle was 0.09°. Figure 8 shows the results when averaged over the six hue angles and Table II shows the data for the individual hue angles.

The noise block resolution that was used in our main Experiments 1 and 2 is indicated in Fig. 8 by the arrow on the horizontal axis (0.58°). It is evident that the thresholds for detection of noise are seriously raised when the noise blocks become smaller, an effect that is predicted by the spatial contrast sensitivity function of the human eye.[18,19] Although Fig. 8 provides a nice overview of the average effect (the thresholds were averaged over the six hue angles), the data in Table II show a more refined picture. For example, the threshold for h at $h = 240$ is always the highest of the six hue angles, in accordance with Fig. 5. Over the resolution range that we tested here, the relative order for the thresholds in L^*, C^*, and h as displayed by Fig. 8 remains unaltered.

DISCUSSION

Comparison with Other Studies

Psychophysical studies on the perception of noise or nonuniformity in visual stimuli have already been

TABLE II. Thresholds for the detection of noise for different sizes of the noise blocks.

Size of noise blocks (°)	Perceptual direction	Hue angle (°) 0	60	120	180	240	300
0.10	*L*	0.153	0.163	0.148	0.146	0.158	0.136
	C	0.715	0.884	1.723	1.156	0.893	1.127
	h	1.422	1.564	1.278	1.089	3.764	1.056
0.29	*L*	0.067	0.109	0.084	0.120	0.146	0.109
	C	0.344	0.209	0.551	0.455	0.436	0.477
	h	0.367	0.595	0.529	0.499	1.076	0.512
0.38	*L*	0.088	0.091	0.089	0.105	0.119	0.076
	C	0.340	0.292	0.577	0.466	0.365	0.568
	h	0.456	0.500	0.447	0.388	1.117	0.370
0.48	*L*	0.081	0.087	0.089	0.082	0.091	0.073
	C	0.264	0.181	0.416	0.368	0.199	0.409
	h	0.209	0.381	0.261	0.355	0.802	0.303
0.58	*L*	0.066	0.084	0.073	0.069	0.083	0.073
	C	0.193	0.181	0.372	0.342	0.239	0.431
	h	0.308	0.380	0.359	0.308	0.869	0.280
0.67	*L*	0.067	0.125	0.070	0.093	0.125	0.088
	C	0.227	0.180	0.297	0.307	0.278	0.397
	h	0.272	0.385	0.329	0.353	0.776	0.242
0.86	*L*	0.082	0.104	0.073	0.102	0.129	0.076
	C	0.296	0.173	0.331	0.366	0.231	0.391
	h	0.266	0.385	0.250	0.280	0.895	0.251
1.63	*L*	0.091	0.123	0.099	0.117	0.141	0.107
	C	0.196	0.183	0.270	0.308	0.270	0.400
	h	0.326	0.392	0.245	0.336	0.690	0.175
4.61	*L*	0.117	0.158	0.093	0.139	0.145	0.163
	C	0.333	0.237	0.580	0.386	0.298	0.563
	h	0.303	0.367	0.279	0.404	0.737	0.329

Data from observer JR, at $L^* = 50$ and $C^* = 20$. In Fig. 8 the data is shown when averaged over the six hue angles.

performed by a number of researchers.[10,11,20–34] The results of these studies are usually analyzed in the context of higher order postreceptoral mechanisms, featuring two opponent chromatic mechanisms and one achromatic (luminance) mechanism. In contrast, we have used the CIE94 color difference formula as our starting point for describing results in a series of experiments in which the detection of noise and the recognition of the orientation of a test symbol were the central issues.

In doing so, we did not fulfill the reference conditions under which CIE94 performs well, and had to change the parametric factors k_L, k_C, and k_H accordingly. For our nonuniform stimuli it became very clear that CIE94 does not support the construction of a perceptual uniform space. Griffin and Sepehri[35] have compared the performance of CIE94 with several other color difference formulae when taking CIE94 out of its preferred reference conditions, and found that subjective color differences were not predicted very well. In our case, we violate the reference conditions mainly with nonuniformity of the colors and with smaller sample sizes. The effect of the latter in particular can be traced to existing literature on wavelength discrimination and so called "small-field-tritanopia" (e.g., McCree[36]). When objects get smaller in angular subtense, our ability to detect them decreases, and this depends on the color (the wavelengths) of the object. Effectively we become blind to small sized colors, the blue ones being the first to "disappear." The fact that blue and small objects are less well visible may at least partly explain the peak threshold for noise in hue at $h = 240°$ (the blue corner of color space). Experiments by Qiao *et al.*[37] who studied three hue circles at two lightness levels and two chroma levels revealed that there is a hue dependency on color-difference tolerances with a maximum near 240°. This closely resembles the results of our Experiment 1. We find hue dependent threshold values for the detection of noise in direction C^*, in line with the work of Melgosa *et al.*,[38] but in addition we also find a hue-dependency of the thresholds in h.

In additional pilot studies (not shown here) using $L^* = 75$ we found that there is a higher average threshold compared to $L^* = 50$. This confirms the results of Montag and Berns[5] who showed that lightness tolerance increases with increasing lightness of the test stimuli. All in all, our data seem to be closely related to earlier work on the development of color difference formulae and chromatic discrimination.

Spectral Opponency of C^* and h

What could be the nature of the opponent hue dependency of the noise detection thresholds in C^* and h? The data curves in Fig. 5 show a systematic opponent behavior, and reveal that the thresholds for C^* and h have four crossings at hue angles of about 90, 180, 285, and 345°. One explanation could be that the curves result somehow from the fact that the human visual system has different contrast sensitivity functions for red-green and blue-yellow modulations.[19] For a given spatial frequency the blue-yellow mechanism has lower contrast sensitivity than the red-green mechanism. So, when varying the hue angle of our stimuli this result in varying stimulations of the two opponent chromatic mechanisms, and hence varying detection thresholds. We have attempted to replot Fig. 5 on a wavelength scale, rather than on the hue angle scale, but because of the spectral composition of the light emitted by the LCD's primaries we can only plot dominant wavelength. Still, this results in a graph that reminds of wavelength discrimination graphs,[39] which plot the amount of $\Delta\lambda$ necessary for discriminating a test patch at wavelength λ from a patch at $\lambda + \Delta\lambda$. However, it remains to be solved how $\Delta\lambda$ transforms into ΔL^*, ΔC^*, Δh.

Spatial Size Effects

The CIE94 reference conditions require sample sizes of at least 4°. From Fig. 8, it follows that our stimulus with noise blocks of 4° is detected at a ΔE^*_{94} threshold of about 0.4 for C^* and h, and about 0.13 for L^*, in both cases substantially lower than the expected reference value $\Delta E^*_{94} = 1$. This is partly explained by the fact that our stimulus is built up by adjacent blocks that maximally differ two times the ΔE^*_{94} threshold value (i.e., a block having the average color plus ΔE^*_{94} bordering a block having the average color minus ΔE^*_{94}), meaning that our threshold values of 0.4 correspond to 0.8 for a difference of 1 ΔE^*_{94} Still, the low detection threshold value for L^* remains noteworthy, even when corrected with the factor of 2.

In one of our pilot experiments, we separated the individual noise blocks by thin black lines. Since in this case the color noise blocks did not border each other but always border a black line (high luminance contrast), we measured a 7-fold increase in the threshold for L^*, and a 2-fold increase in the threshold for C^*. This effect is well known—and greatly appreciated—in the car refinishing industry. When two car panels (two doors on one side of the vehicle for example) are separated by a dark strip, the tolerance for the color difference between the two panels is doubled,[40] which makes a panel repair somewhat less difficult.

Alternative Data Descriptions

We presented our experimental data in terms of the ΔE^*_{94} metric, but we realize that there may be more convenient ways to analyze the data. Ideally one would like to obtain a description of the data that resembles the situation illustrated by the top panel in Fig. 6, i.e., an orthogonal space in which there is a single response to a single variable. We have roughly explored the usefulness of data analyses in terms of LMS cone excitations and cone contrasts, and further analysis in DKL color space.[41] Also we have tried the line element theory,[42] but so far we have not improved on our analysis in L^*, C^*, and h.

Presentation of these data analyses would require too much space in this article. Moreover, we feel that more experimental data should be collected and analyzed before drawing conclusions about the most suitable space for describing the data and the behavior of the visual system. It seems that when we stick to three perceptual "channels" (low or high level), interactions between these channels remain. One alternative that needs to be researched is the use of multiple broadly tuned chromatic detection mechanisms, as described in Ref. 33.

Absolute Versus Relative Color Accuracy

The average absolute accuracy with which colors can be reproduced on our display was determined to be in the order of $\Delta E^*_{94} = 0.6$. However, most of the measured detection thresholds are below that value. This may seem contradictory, but it is simply caused by the difference between *absolute* and *relative* color accuracy. The color reproduction accuracy relates to the absolute color difference between desired (target) colors and colors actually produced on the display, which can be measured by an instrument to quantify that difference. The detection threshold, however, is determined by visual assessment of the stimuli, which in essence is a comparison of small differences between adjacent stimulus areas, i.e., a relative measurement.

Implications for Practice

In the Introduction section, we already mentioned the relevance of our study for the design of color vision tests and false-color imaging in multi sensor applications. In the latter it may be envisaged that two or more images from different sensors are combined into a single false-color image in a way that maximizes the detection of a target object. Let us consider the case with two imaging sensors in different spectral bands, resulting in two images with different signal to noise (*S*/*N*) ratios. In the case that one image has a considerable higher *S*/*N* than the other, the results shown in Fig. 7 then suggest to display the image from the sensor with the higher *S*/*N* in the C^* or h domain (having the lowest detection threshold). When both sensors produce high *S*/*N* images fusion is worthwhile because of the difference in spectral information. When both sensors produce low *S*/*N* images fusion may also be worthwhile to improve on the *S*/*N* of a separate image.

Another application of our results could be the improvement of image quality by intelligent noise reduction. Related to that topic is optimized color quantization for compression purposes. Last but not least, we mention the potential for improvement of industrial color difference equations. Our experimental method is one that required a lot of attention to the details of display characterization, color accuracy, and selection, but can be performed on an ordinary personal computer with high quality LCD or CRT monitor.

ACKNOWLEDGMENTS

The authors thank Dr. J. J. Vos for commenting on an earlier draft of this article and pointing out the potential benefit of using line-element theory for describing their data.

APPENDIX

This appendix deals with three technical issues. The first relates to the colorimetric calibration of the LCD monitor that was used for presenting the stimuli. We report on the absolute accuracy with which we were able to reproduce specified colors on the display. The second topic is the spatial dithering technique that we used to increase the color resolution of our system from the standard 24 bit to 33 bits. We experimentally verified that the spatial dithering did not induce perceptual artifacts. The third topic deals with the problem of selecting the most suitable color from the discrete RGB gamut that yields the desired color difference (ΔL^*, ΔC^*, Δh) with a target color.

Colorimetric Calibration of the LCD

During the period in which we performed the experiments we kept our LCD monitor at maximum white luminance of 120 cd/m^2, a white point of 6500 K, and gamma 2.2 for each of the three primary channels. This was done using a GretagMacbeth Eye-One spectrophotometer and software by Eizo, enabling hardware self-calibration of the LCD. Before each experimental run, the LCD was self-calibrated at the target settings mentioned earlier. Full colorimetric characterization of the display at these settings was performed using a Photo Research PR-650 spectrophotometer. We followed the procedure as described by Cazes *et al.*[43] These authors propose a method in which the common color calibration model for a CRT (e.g., Berns *et al.*[44]) is modified to characterize the LCD. The modifications account for the relatively high luminance of black (sub) pixels and color leakage from bright to dark subpixels in LCDs. For a detailed description, we refer to Ref. 43. In short, we measured the 2° *XYZ* values for 33 drive values (including 0 and 255) on the red, green, and blue channels separately, and simultaneously (producing grey). Next, the *XYZ* values of black subpixels and the color leakage are computed from the measurements, and these are modified such that the red, green, and blue channel add up to the "grey channel" (additivity check). As a result, the chromaticities of the primaries are almost independent of the intensity level. For our display, the CIE x, y chromaticities of the red, green, and blue primaries are (0.641, 0.329), (0.289, 0.598), and (0.143, 0.065), respectively. In Fig. 9 the original luminance data (left) and modified data (right) are shown. The modifications are best noticeable at the lower drive values. Note that the graphs are on a log-log scale, implying that the slopes of the curves correspond to the gamma values of

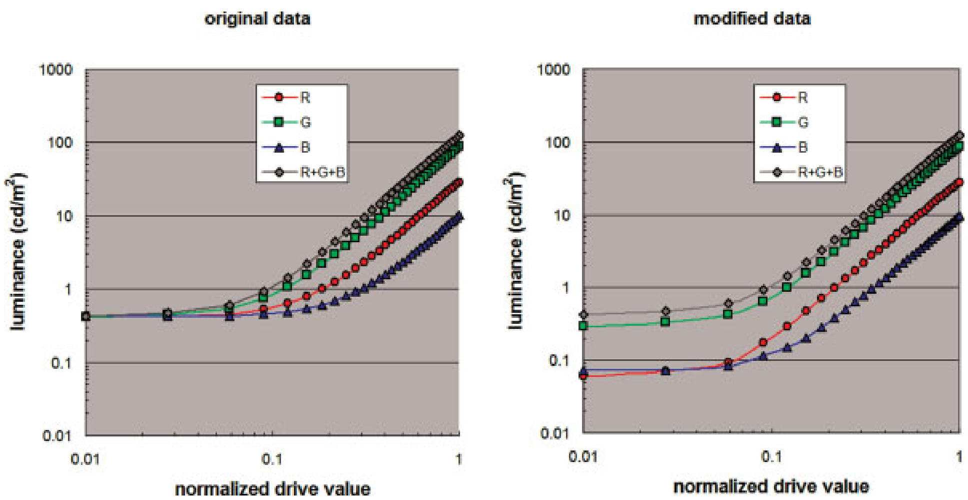

FIG. 9. Luminance measured from the LCD as a function of the normalized drive value. Left panel shows the original luminance data, the panel on the right hand side the modified data as obtained with the method by Cazes *et al.*[43] resulting in independent primary channels, as is best visible at the lower drive values. The most left data point belongs to drive value 0, but is drawn here at normalized drive value 0.01. [Color figure can be viewed in the online issue, which is available at www.interscience.wiley.com.]

the primary channels and that of the "grey channel." From the plots in Fig. 9, it can be derived that the target gamma value of 2.2 is indeed obtained.

When generating a color specified in X, Y, Z (2° observer) on the display, the required luminances from the red, green, and blue channel, here indicated with Y_R, Y_G, Y_B, were calculated with the inverse of

$$\begin{pmatrix} X \\ Y \\ Z \end{pmatrix} = \begin{pmatrix} x_R/y_R & x_G/y_G & x_B/y_B \\ 1 & 1 & 1 \\ z_R/y_R & z_G/y_G & z_B/y_B \end{pmatrix} \begin{pmatrix} Y_R \\ Y_G \\ Y_B \end{pmatrix} \quad \text{(A1)}$$

in which the nine matrix elements are computed by entering the x, y, z chromaticities of the LCD primaries. Finally, the R, G, B drive values required for generating the desired Y_R, Y_G, Y_B luminances are derived from interpolation of the luminance curves shown in Fig. 9. For curves as shown in Fig. 9, linear interpolation on a log-log basis has been shown to be more accurate than interpolation on a linear scale.[45] To test the accuracy of our calibration procedure, we randomly selected 50 test colors within the display's color gamut, generated these on our display [using Eq. (A1)], and measured the colors as produced on the LCD. Measurements were made with the PR-650 at 50 cm distance, perpendicular to the center of the screen. The 50 test colors were shown at the center of the screen, in size 1/5 of the width and height of the full screen background which was presented at mid gray ($R = G = B = 128$). We obtained an average difference between estimated and measured colors of $\Delta E^*_{94} = 0.64$ (min = 0.15, max = 1.15). In terms of the CIEDE2000 color difference formula the average difference is $\Delta E_{00} = 0.62$ (min = 0.14, max = 1.29). Compared to the performance on LCD characterization reported by Day *et al.*[46] this is less accurate than their best results with one particular monitor (ΔE_{00} = 0.1–0.4), but more accurate than their results for three additional monitors (ΔE_{00} = 0.7–1.8).

Low Contrast Dithering to Increase Color Resolution

Initial pilot experiments revealed—as expected—that the standard 24-bit RGB resolution of our computer's graphics card in combination with our display settings was not adequate for accurate measurement of the lowest visual thresholds (in terms of ΔL^*, ΔC^*, and ΔH^*) we were studying. We, therefore, increased the RGB resolution in software to 33 bits at the cost of spatial resolution, a technique known as color dithering. Each block of 3 × 3 pixels was treated as one "super pixel." Up to 8 of the 9 pixels within one such super pixel could be addressed with an R, G, B drive value that was identical to or one count higher in drive value than the remaining pixel(s). Averaged over the super pixel area this leads to eight additional intervals (3 bits) in between two integer drive values, within each of the three R, G, B channels. For example, setting the R drive value of 1 pixel to 121 while the other 8 pixels of the super pixel remain at a value of 120, the average becomes (121 + 8 × 120) / 9 = 120.11. Setting 2 pixels at 121, the average becomes (2 × 121 + 7 × 120) / 9 = 120.22, and so on. In Fig. 10 an example is provided demonstrating how the increased resolution in R, G, B drive values leads to an increase in L^*, C^*, h resolution.

In the example of Fig. 10 the target color was $L^* = 50$, $C^* = 20$ and $h = 0$ and is located in the origin. According to our display characterization, drive values of $R = 145$, $G = 105$, $B = 117$ most closely approximated this target color. Figure 10 shows how steps in L^*, C^*, h can be created when varying the drive values around $R = 145$, $G = 105$, $B = 117$, either with step size 1 (24-bit resolution, left panels) or 1/9 (33-bit resolution, right

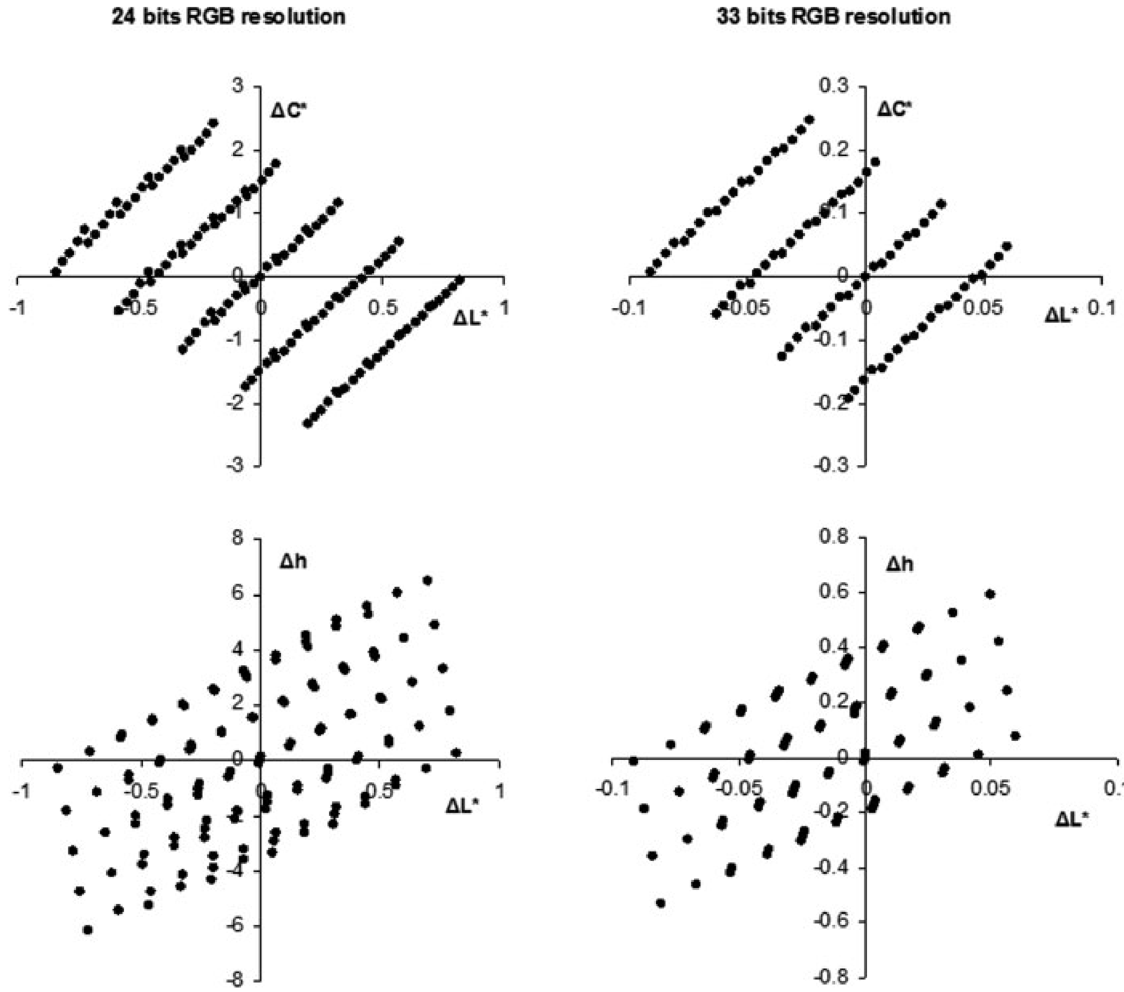

FIG. 10. Improvement in color resolution when going from standard 24 bits (left panels) to 33 bits (right panels) in RGB space, which was obtained in software (see text). Top panels show ΔL^*, ΔC^* space with its origin at $L^* = 50$, $C^* = 20$; the bottom panels show ΔL^*, Δh space with its origin at $L^* = 50$, $h = 0$. Note that the scale of the right panels is one-tenth of the scale of the left panels. The data points were obtained by varying R, G, B drive values around $R = 145$, $G = 105$, $B = 117$ (corresponding to the origin in the plots), either in steps of one (24-bit resolution) or in steps of 1/9 (33-bit resolution).

panels). For example, the smallest step in ΔL^* with respect to the center color while keeping ΔC^* zero is about 0.41 in the case of 24 bit and 0.045 in the case of 33-bit color resolution (note the different scales for the left and right panels in Fig. 10).

Experimental Verification. We experimentally verified that the low contrast color dithering did not induce some kind of visual artifact. For the 3 pixels along one diagonal of each 3×3 super pixel we increased the G drive value with steps of three, resulting in an increase of the 3×3 pixel average in steps of one. The G drive value was initially 150, while R and B were zero. As shown in Fig. 9, the displays' G-channel stimulates luminance most significantly. With the diagonal pixels intensified, a visual artifact may become visible because of the repetitive luminance pattern that is created for larger blocks of super pixels. We selected the G-channel for this experiment because we expected a luminance pattern to be better detected than a chromatic pattern, and thus would provide us with a more critical test. In a 4-AFC setup similar to our Experiment 1 and 2, five subjects were asked to indicate which quadrant contained the super pixels with intensified diagonal, and to indicate when they were guessing. The target quadrant consisted of a checkerboard pattern of blocks of super pixels intensified along three diagonal pixels and blocks of super pixels intensified in all 9 pixels to be equiluminant with the former. This restricts the diagonal offset to multiples of three. Figure 11 shows how the number of guesses increases when the diagonal offset in luminance is decreased to a value of three, the lowest value that could be tested in this way. It also shows that when extrapolating the data to an increase of 1 count in drive value—as actually used in our experiments—the percentage correctly recognized quadrants drops to an $\sim$25%, i.e., at the guessing level indicated by the dashed horizontal line. We conclude from these measurements that dithering by 1 count in drive value in blocks of 3×3 pixels is not inducing visual artifacts in our stimuli. Baribeau and Robertson[47] have also recently reported on hue-threshold measurements on computer

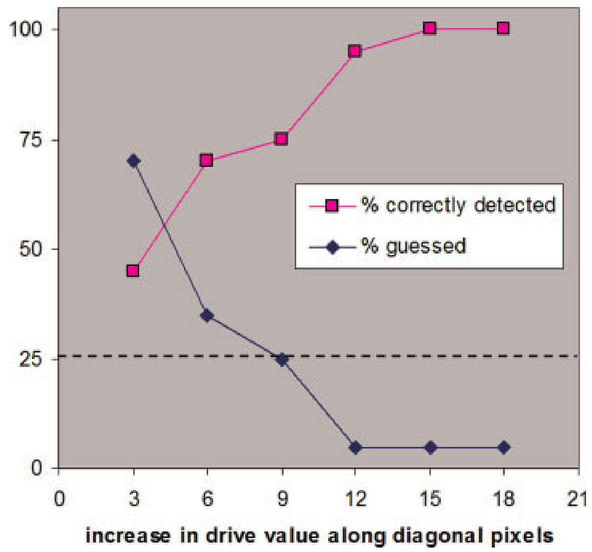

FIG. 11. Percentage correctly recognized quadrant containing a luminance intensified diagonal in the super pixel (block of 3 × 3 pixels) as a function of the luminance increase in terms of *G* drive value. For increases in multiples of three, the average over a super pixel is increased in multiples of one. When extrapolating the data to an increase of one count in drive value, the percentage correctly recognized approximates 25%, i.e., at the guess level indicated by the dashed horizontal line. Data from five observers, each data point represents 20 measurements. [Color figure can be viewed in the online issue, which is available at www.interscience.wiley.com.]

display, using dithering on blocks of 2 × 2 pixels to improve color resolution with 2 bits per primary channel.

Criterion for Color Selection

In our experiments, we want to measure visual thresholds in terms of ΔL^*, ΔC^*, and ΔH^*. We make use of a staircase procedure that adjusts the strength of the color signal in one direction (L^*, C^*, or h) while maintaining the other two fixed. Unfortunately, this cannot always be realized with a sufficiently small ΔE step in the desired direction, given the discrete steps in ΔL^*, ΔC^*, Δh space as shown in Fig. 10 for one target color example. We, therefore, designed a color selection criterion with which we could search for the best among ΔL^*, ΔC^*, Δh alternatives. First, the color difference ΔE^*_{94} between the target color and neighboring L^*, C^*, h grid points was calculated. To have a large enough pool of neighboring points we evaluated 16,6375 (=55^3) variations in RGB around the target color (we arrived at this number by trial and error). For those with a computed color difference below 10% of the desired color difference $\Delta E_{\mathrm{target}}$, the "dominance factor" (DF) of the components ΔL^*, ΔC^*, ΔH^* in ΔE_{94} was determined, i.e., their relative contribution to ΔE^*_{94}, as in

$$DF_L = \left(\frac{1}{\Delta E^*_{94}}\frac{\Delta L^*}{S_L k_L}\right)^2 \tag{A2}$$

$$DF_C = \left(\frac{1}{\Delta E^*_{94}}\frac{\Delta C^*}{S_C k_C}\right)^2 \tag{A3}$$

$$DF_H = \left(\frac{1}{\Delta E^*_{94}}\frac{\Delta H^*}{S_H k_H}\right)^2 \tag{A4}$$

The DFs indicate how "dominant" the components ΔL^*, ΔC^*, and ΔH^* are with respect to the total color difference ΔE^*_{94}. Note that the three DFs add up to 1. We required a minimum value of 0.9 for the DF. For each candidate color, we then computed a score defined as

$$\mathrm{score} = 0.25(1 - \mathrm{DF}) + |\Delta E^*_{94} - \Delta E_{\mathrm{target}}| \tag{A5}$$

and selected the color with the lowest score as our final color. The rationale behind the score is that the higher the DF, the better the candidate color suits the desired direction of color change. However, a candidate color with a DF of 1 is not necessarily the "best color," since its associated color difference (ΔE^*_{94}) may be too far off the desired color difference ($\Delta E_{\mathrm{target}}$). Therefore, any mismatch between ΔE^*_{94} and $\Delta E_{\mathrm{target}}$ is penalized in the computation of the score [Eq. (A5)], four times as heavily as a mismatch in the DF. Since the DF may vary between 0.9 and 1, the value of 0.25 (1−DF), the first term in Eq. (A5), is restricted to a maximum of 0.025. The second term in Eq. (A5), $|\Delta E^*_{94} - \Delta E_{\mathrm{target}}|$ is always $<0.1\Delta E_{\mathrm{target}}$. Analysis of our pilot data showed that for the measurement of the smallest thresholds (those associated with noise in L^*), $\Delta E_{\mathrm{target}}$ is in the order of 0.1, and thus $|\Delta E^*_{94} - \Delta E_{\mathrm{target}}| < 0.01$. For those—most critical—situations, the value of the DF is most significant for the color selection.

1. CIE. Colorimetry, 2nd edition. CIE Publication No. 15.2. Vienna: Central Bureau of the CIE, 1986.
2. Clarke FJJ, McDonald R, Rigg B. Modification to the JPC79 colour difference formula. J Soc Dyers Col 1984;100:128–132.
3. CIE Pub, 116-1995. Industrial Colour-Difference Evaluation. Vienna: CIE Central Bureau; 1995.
4. CIE Pub, 142-2001. Improvement to Industrial Colour-Difference Evaluation. Vienna: Central Bureau; 2001.
5. Montag ED, Berns RS. Lightness dependencies and the effect of texture on suprathreshold lightness tolerances. Color Res Appl 2000;25: 241–249.
6. Xin JH, Shen HL, Lam CC. Investigation of texture effect on visual colour difference evaluation. Color Res Appl 2005;30:341–347.
7. Huertas R, Melgosa M, Hita E. Parametric factors for colour differences of samples with simulated texture. AIC Colour 05–10th Congress of the International Colour Association, Granada, Spain; 2005.
8. Johnson GM, Fairchild MD. A top down description of S-CIELAB and CIEDE 2000. Color Res Appl 2003;28:425–435.
9. Dain SJ. Clinical color vision tests. Clin Exp Optom 2004;87:276–293.
10. Driggers RG, Krapels K, Vollmerhausen R, Warren P, Scribner D, Howard G, Tsou BH, Krebs WK. Target detection thresholds in noisy color imagery. SPIE Proc 2001;4372:162–169.
11. Krapels K, Jones T, Driggers RG, Teany B. Target detection in color imagery: On the path to a color target acquisition model. SPIE Proc 2004;5612:295–303.

12. Lucassen MP, Bijl P. The CIE94 color difference formula for describing visual detection thresholds in static noise. Second European Conference on Color in Graphics, Imaging and Vision, Aachen, Germany, 2004. pp 8–11.
13. Bijl P, Lucassen MP, Roelofsen J. Infrared Imaging Systems: Design, Analysis, Modeling, and Testing XVI. In: Gerald C. Holst, editors. Proceedings of SPIE, SPIE Digital Library, Vol. 5784. 2005. pp 35–41.
14. Bijl P, Toet A, Valeton JM. Psychophysics and psychophysical measurement procedures. Encyclopedia Opt Eng 2003:2176–2187.
15. Levitt H. Transformed up-down methods in psychoacoustics. J Acoust Soc Am 1971;49:467–477.
16. Walraven J, Lucassen MP, Alferdinck JWAM, Kooi FL. Automated visual screening; development of computerised vision tests for the TNO VisionScreener, TNO-report TM-02-A044. 2002.
17. Luo MR, Cui G, Rigg GCB. The development of the CIE 2000 color-difference formula: CIEDE 2000. Color Res Appl 2001;26: 340–350.
18. Kelly DH. Spatiotemporal variation of chromatic and achromatic contrast thresholds. J Opt Soc Am 1983;73:742–750.
19. Fairchild MD. Color Appearance Models. Reading, MA: Addison-Wesley; 1998.
20. Moorhead IR, Saunders JE. Discrimination and dectection thresholds: The effect of observer criterion on the spatial properties of chromatic and achromatic mechanisms. Vision Res 1982;22:1057–1062.
21. Legge GE, Kersten D, Burgess AE. Contrast discrimination in noise. J Opt Soc Am A 1987;4:391–404.
22. Switkes E, Bradley A, De Valois KK. Contrast dependence and mechanisms of masking interactions among chromatic and luminance gratings. J Opt Soc Am A 1988;5:1149–1162.
23. Gegenfurtner KR, Kiper DC. Contrast detection in luminance and chromatic noise. J Opt Soc Am A 1992;9:1880–1888.
24. Poirson AB, Wandell BA. Appearance of colored patterns: Pattern-color separability. J Opt Soc Am A 1993;10:2458–2470.
25. Poirson AB, Wandell BA. Pattern-color separable pathways predict sensitivity to simple colored patterns. Vision Res 1996;35:239–254.
26. Yaguchi H, Masuda I, Shiori S, Miyake Y. Analysis of the color discrimination data in the physiological based color space. Die Farbe 1993;39:105–114.
27. Li A, Lennie P. Mechanisms underlying segmentation of colored textures. Vision Res 1997;37:83–97.
28. Sankeralli MJ, Mullen, KT. Postreceptoral chromatic detection mechanisms revealed by noise masking in three-dimensional cone contrast space. J Opt Soc Am A 1997;14:2633–2646.
29. D'Zmura M, Knoblauch K. Spectral bandwidths for the detection of color. Vision Res 1998;38:3117–3128.
30. Ahumada AJ, Krebs WK. Signal detection in fixed pattern chromatic noise. Invest Ophthalmol Vis Sci 2000;41:3796–3804.
31. Levi DM, Klein SA, Chen I. What is the signal in noise? J Vis 2004;4:49a.
32. Hansen T, Gegenfurtner KR. Classification images for chromatic signal detection. J Opt Soc Am A 2005;22:2018–2089.
33. Hansen T, Gegenfurtner KR. Higher level chromatic mechanisms for image segmentation. J Vis 2006;6:239–259.
34. Monaci G, Menegaz G, Susstrunk S, Knoblauch K. Chromatic contrast detection in spatial chromatic noise. Vis Neurosci 2004;21:291–294.
35. Griffin LD, Sepehri A. Performance of CIE94 for non-reference conditions. Col Res Appl 2002;27:108–115.
36. McCree KJ. Small-field tritanopia and the effects of voluntary fixation. Opt Acta (Lond) 1960;7:317–323.
37. Qiao Y, Berns RS, Reniff L, Montag E. Visual determination of hue suprathreshold color-difference tolerances. Col Res Appl 1998;23: 302–313.
38. Melgosa M, Huertas R, Yebra A, Pérez MM. Are chroma tolerances dependent on hue-angle? Col Res Appl 2004;29:420–427.
39. Walraven PL, Bouman MA. Fluctuation theory of colour discrimination of normal trichromats. Vision Res 1966;6:567–586.
40. DIN 6175. Color tolerances for vehicle paints, Part 1: Plain paints. 1986.
41. Derrington AM, Krauskopf J, Lennie P. Chromatic mechanisms in the lateral geniculate nucleus of macaque. J Physiol 1984;357:241–265.
42. Vos JJ. From lower to higher color metrics, a historical account. Clin Exp Optom 2006;89:348–360.
43. Cazes A, Braudaway G, Christensen J, Cordes M, DeCain D, Lien A, Mintzer F, Wright SL. On the color calibration of liquid crystal displays. Proc IS and T/SPIE Conference on Display Metrology, San Jose; 1999. pp 154–161.
44. Berns RS, Motta RJ, Gorzynski ME. CRT colorimetry, Part I: Theory and practice. Color Res Appl 1993;18:299–314.
45. Lucassen MP, Walraven J. Evaluation of a simple method for color monitor recalibration. Color Res Appl 1990;15:321–326.
46. Day EA, Taplin L, Berns RS. Colorimetric characterization of a computer-controlled liquid crystal display. Color Res Appl 2004;29: 365–373.
47. Baribeau R, Robertson AR. Estimation of hue discrimination thresholds using a computer interactive method. Color Res Appl 2005; 30:410–415.